Large inflationary logarithms in a nontrivial nonlinear sigma model

C. Litos,* R. P. Woodard,† and B. Yesilyurt‡

Department of Physics, University of Florida, Gainesville, Florida 32611, USA

(Received 28 June 2023; accepted 18 August 2023; published 7 September 2023)

Loops of inflationary gravitons are known to induce large temporal and spatial logarithms that can cause perturbation theory to break down. Nonlinear sigma models possess the same kind of derivative interactions and induce the same sorts of large logarithms, without the complicated index structure and potential gauge problem. Previous studies have examined models with zero field space curvature that can be reduced to free field theories by local, invertible field redefinitions. Here we study a model that cannot be so reduced and still shows the same sorts of large logarithms. We compute the evolution of the background at 1-loop and 2-loop orders, and we find the 1-loop β and γ functions.

DOI: 10.1103/PhysRevD.108.065001

I. INTRODUCTION

The background geometry of cosmology is characterized by scale factor $a(t)$, Hubble parameter $H(t)$, and first slow-roll parameter $\epsilon(t)$,

$$ds^2 = -dt^2 + a^2(t)d\vec{x}\cdot d\vec{x} \quad \Rightarrow \quad H(t) \equiv \frac{\dot{a}}{a},$$
$$\epsilon(t) \equiv -\frac{\dot{H}}{H^2}. \tag{1}$$

The accelerated expansion of inflation [$H(t) > 0$ with $0 \leq \epsilon(t) < 1$] rips virtual scalars and gravitons out of the vacuum. This is the basis for the primordial spectra of scalars [1] and tensors [2]. At some level these quanta must interact among themselves and with other particles. Gravitons are especially interesting because their couplings are universal and because their tensor structure allows them to mediate effects which scalars cannot. For example, on de Sitter background [$\epsilon(t) = 0$] 1-loop gravitons modify the plane wave mode function $u(t,k)$ of gravitational radiation [3] and the gravitational response $\Psi(t,r)$ to a point mass [4] to

$$u(t,k) = u_0(t,k)\left\{1 + \frac{16GH^2}{3\pi}\ln^2(a) + O(G^2)\right\}, \tag{2}$$

$$\Psi(t,r) = -\frac{GM}{ar}\left\{1 + \frac{103G}{15\pi a^2 r^2} - \frac{8GH^2}{\pi}\ln^3(a) + O(G^2)\right\}. \tag{3}$$

Similar results have been obtained for the corrections of inflationary gravitons to fermions [5], to electrodynamics [6,7], and to massless, minimally coupled scalars [8].

A fascinating aspect of these corrections is that the steady production of inflationary gravitons endows them with a secular growth which must eventually overwhelm the loop-counting parameter GH^2 provided inflation persists long enough. One must develop a nonperturbative resummation technique in order to evolve past that point. Nonlinear sigma models provide a useful testing ground for developing such a technique because they possess the same sorts of derivative interactions as gravitons, and induce the same sorts of large logarithms, without the complicating tensor structures or the potential for gauge dependence [9–12]. A successful technique has been devised through combining a variant of Starobinsky's stochastic formalism [13,14] with a variant of the renormalization group [15,16]. Even better, the technique can be generalized from de Sitter to an arbitrary cosmological background (1) which has undergone primordial inflation [17]. Applying this technique shows that the large scales of primordial inflation can be transmitted to late time [18].

The obvious next step is generalizing the resummation technique from nonlinear sigma models to quantum gravity. This seems to be entirely possible and works for the one graviton loop correction on which it has been checked [8]. However, our purpose here is to clear up a worry concerning the sorts of nonlinear sigma models on which the resummation technique has so far been applied. Specifically, both of those models can be reduced to free theories by means of local invertible field redefinitions, which means that their flat space S-matrices are unity by Borchers theorem [19]. That in no way precludes interesting evolutions for the scalar backgrounds and for the 1-particle states, and it was these evolutions which suggested and confirmed the resummation technique. One might still worry that the technique

*c.litos@ufl.edu
†woodard@phys.ufl.edu
‡b.yesilyurt@ufl.edu

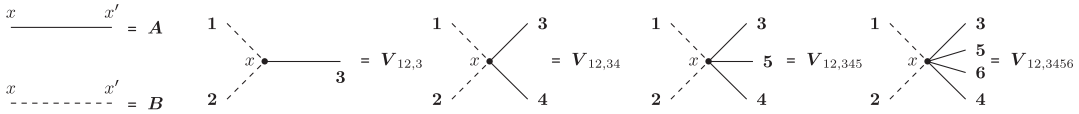

FIG. 1. Primitive interactions of the bare Lagrangian (8). A lines are solid and B lines are dashed.

only works for models which can be reduced to free theories. The purpose of this paper is to demonstrate that the resummation technique applies for a model whose flat space S-matrix is nontrivial.

This paper contains five sections, of which this Introduction is the first. In Sec. II we describe the old and new models, and we give the Feynman rules. Section III computes the time-evolving background at 1-loop and 2-loop orders. It also computes and renormalizes the one-particle-irreducible (1PI) 2-point and 3-point functions at 1-loop order. The resummation technique is applied in Sec. IV. Our conclusions comprise Sec. V.

II. THE MODEL

The purpose of this section is to define the model and give those of its Feynman rules that are required for our work. We begin by presenting the old models and explaining why their S-matrices are trivial. Then a new model is proposed by making a small variation that preserves the lowest order interactions.

The resummation technique was developed based on work with two nonlinear sigma models [15]. One of these was based on a single field. All models of this sort can be made free by a local, invertible field redefinition,

$$\mathcal{L} = -\frac{1}{2} f^2(\Phi) \partial_\mu \Phi \partial_\nu \Phi g^{\mu\nu} \sqrt{-g},$$
$$d\Psi \equiv f(\Phi) d\Phi \quad \Rightarrow \quad \mathcal{L} = -\frac{1}{2} \partial_\mu \Psi \partial_\nu \Psi g^{\mu\nu} \sqrt{-g}. \tag{4}$$

A second model was based on two fields,

$$\mathcal{L}_{\rm old} = -\frac{1}{2} \partial_\mu A \partial_\nu A g^{\mu\nu} \sqrt{-g} - \frac{1}{2} \left(1 + \frac{\lambda}{2} A\right)^2 \partial_\mu B \partial_\nu B g^{\mu\nu} \sqrt{-g}. \tag{5}$$

Although it was not initially realized, this model can also be reduced to a theory of two free scalars by making a local, invertible field redefinition,[1]

$$X \equiv \frac{2}{\lambda} \left(1 + \frac{\lambda}{2} A\right) \cos\left(\frac{\lambda}{2} B\right), \tag{6}$$

$$Y \equiv \frac{2}{\lambda} \left(1 + \frac{\lambda}{2} A\right) \sin\left(\frac{\lambda}{2} B\right). \tag{7}$$

[1]We thank Arkady Tseytlin for this observation.

Hence the flat space S-matrices of (4) and (5) are both unity by Borchers theorem [19]. That in no way precludes these models from manifesting interesting evolutions of their backgrounds and of the single-particle kinematics.

To be certain that the resummation technique does not rely on having a trivial S-matrix we devised a slight modification of the 2-field model (5) whose field space curvature implies that it cannot be reduced to a fee theory,

$$\mathcal{L}_{\rm new} = -\frac{1}{2} \partial_\mu A \partial_\nu A g^{\mu\nu} \sqrt{-g} - \frac{1}{2} \left(1 + \frac{\lambda}{4} A\right)^4 \partial_\mu B \partial_\nu B g^{\mu\nu} \sqrt{-g}. \tag{8}$$

The 3-point coupling in this model is identical to that of the old model (5), and the 4-point coupling has the same field content with the old numerical coefficient of $\frac{1}{8}$ replaced by $\frac{3}{16}$. There are additional 5-point and 6-point interactions which make only simple contributions to the diagrams we evaluate in Sec. III,

$$\frac{1}{2} \left(1 + \frac{\lambda}{4} A\right)^4 (\partial B)^2 - \frac{1}{2} (\partial B)^2 = \frac{\lambda}{2} A (\partial B)^2 + \frac{3\lambda^2}{16} A^2 (\partial B)^2 + \frac{\lambda^3}{32} A^3 (\partial B)^2 + \frac{\lambda^4}{512} A^4 (\partial B)^2. \tag{9}$$

A diagrammatic representation of the Feynman rules is shown in Fig. 1.

The new model (8) is no more renormalizable than the old one (5). Hence divergences must be subtracted, order-by-order, using Bogoliubov-Parasiuk-Hepp-Zimmermann (BPHZ) counterterms [20–23]. The 1-loop counterterms we require are shown in Fig. 2. The first and second diagrams renormalize the A and B self-masses and correspond to the counterterm,

$$\Delta\mathcal{L}^{(2)} = -\frac{1}{2} C_{1A^2} \Box A \Box A \sqrt{-g} - \frac{1}{2} C_{2A^2} R \partial_\mu A \partial_\nu A g^{\mu\nu} \sqrt{-g} - \frac{1}{2} C_{1B^2} \Box B \Box B \sqrt{-g} - \frac{1}{2} C_{2B^2} R \partial_\mu B \partial_\nu B g^{\mu\nu} \sqrt{-g}. \tag{10}$$

The third diagram is required to renormalize the 3-point vertex and corresponds to

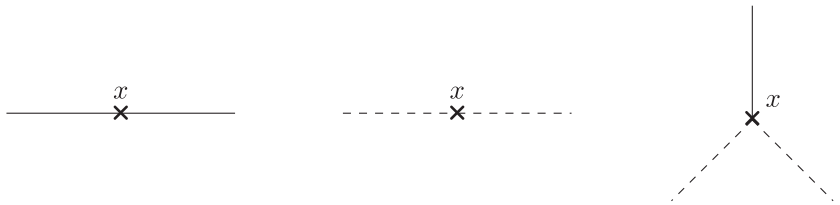

FIG. 2. Diagrammatic representation of the 1-loop counterterms we require. The first two diagrams renormalize the A and B self-masses while the rightmost diagram renormalizes the vertex function. Recall that A lines are solid and B lines are dashed.

$$\begin{aligned}\delta\mathcal{L}^{(3)} =& -\frac{1}{2}C_{1AB^2}\Box A\partial_\mu B\partial_\nu B g^{\mu\nu}\sqrt{-g}\\ &- C_{2AB^2}\partial_\mu A\partial_\nu B\Box B g^{\mu\nu}\sqrt{-g}\\ &-\frac{1}{2}C_{3AB^2}A\Box B\Box B\sqrt{-g}\\ &-\frac{1}{2}C_{4AB^2}RA\partial_\mu B\partial_\nu B g^{\mu\nu}\sqrt{-g}. \end{aligned} \tag{11}$$

Here $R = D(D-1)H^2$ is the Ricci scalar. Section III will determine the various coefficients in expressions (10) and (11) as functions of λ, D, and the dimensional regularization scale μ.

In D spacetime dimensions, the propagators of both fields obey the equation

$$\partial^\mu[a^{D-2}\partial_\mu i\Delta(x;x')] \equiv \mathcal{D}i\Delta(x;x') = i\delta^D(x-x'). \tag{12}$$

The solution consists of a de Sitter invariant part plus a de Sitter breaking logarithm [24,25],

$$\begin{aligned} i\Delta(x;x') &= F(\mathcal{Y}(x;x')) + k\,\ln(aa'),\\ k &\equiv \frac{H^{D-2}}{(4\pi)^{D/2}}\frac{\Gamma(D-1)}{\Gamma\left(\frac{D}{2}\right)}. \end{aligned} \tag{13}$$

Here $\mathcal{Y}(x;x') \equiv aa'H^2\Delta x^2(x;x') \equiv aa'H^2(x-x')^2$ is the de Sitter length function, and the first derivative of $F(\mathcal{Y}(x;x'))$ obeys

$$\begin{aligned} F'(\mathcal{Y}) =& -\frac{H^{D-2}}{4(4\pi)^{D/2}}\left\{\Gamma\left(\frac{D}{2}\right)\left(\frac{4}{\mathcal{Y}}\right)^{\frac{D}{2}} + \Gamma\left(\frac{D}{2}+1\right)\left(\frac{4}{\mathcal{Y}}\right)^{\frac{D}{2}-1}\right.\\ &+\sum_{n=0}^{\infty}\left[\frac{\Gamma\left(n+\frac{D}{2}+2\right)}{\Gamma(n+3)}\left(\frac{\mathcal{Y}}{4}\right)^{n-\frac{D}{2}+2}\right.\\ &\left.\left.-\frac{\Gamma(n+D)}{\Gamma\left(n+\frac{D}{2}+1\right)}\left(\frac{\mathcal{Y}}{4}\right)^{n}\right]\right\}. \end{aligned} \tag{14}$$

In dimensional regularization the coincidence limits of the propagator and its derivatives are

$$\begin{aligned} i\Delta(x;x) &= k\left[-\pi\,\cot\left(\frac{D\pi}{2}\right) + 2\,\ln(a)\right],\\ \partial_\mu i\Delta(x;x')\Big|_{x=x'} &= kHa\delta^0{}_\mu, \end{aligned} \tag{15}$$

$$\begin{aligned} \partial_\mu\partial'_\nu i\Delta(x;x')|_{x'=x} &= -\left(\frac{D-1}{D}\right)kH^2 g_{\mu\nu},\\ \partial_\mu i\Delta(x;x) &= 2kHa\delta^0{}_\mu. \end{aligned} \tag{16}$$

We close by commenting on notation. Because the de Sitter metric $g_{\mu\nu} = a^2\eta_{\mu\nu}$ is conformal to the Minkowski metric $\eta_{\mu\nu}$, we adopt a notation where ∂_μ stands for $\frac{\partial}{\partial x^\mu}$, no matter what sort of tensor it acts upon. Further, we raise and lower its indices using the Minkowski metric, $\partial^\mu \equiv \eta^{\mu\nu}\partial_\nu$. And we define $\partial^2 \equiv \eta^{\mu\nu}\partial_\mu\partial_\nu$. To save space we sometimes write coordinate arguments of the metric and its scale factor using a subscript or a superscript, as in $\sqrt{-g(x)} \equiv \sqrt{-g_x} \equiv a_x^D$ and $g^{\mu\nu}(y) \equiv g_y^{\mu\nu} \equiv a_y^{-2}\eta^{\mu\nu}$. The same notation applies to derivatives, as in $\frac{\partial}{\partial z^\mu} \equiv \partial_\mu^z$.

III. EXPLICIT RESULTS

The purpose of this section is to carry out the same explicit calculations for (8) that were done for the old model (5) [15,16]. We begin with the 1-loop and 2-loop expectation values of $A(x)$. Next, the self-masses of A and B are computed and renormalized at 1-loop order. Finally, we evaluate the 1-loop vertex function.

A. The 1-loop and 2-loop background

We start with the 1-loop expectation value of $A(x)$ whose diagrammatic representation is shown in Fig. 3. Because the 3-point couplings of the old and new models agree, this diagram is unchanged from the old result [15],

FIG. 3. The 1-loop contribution to the expectation value of $A(x)$.

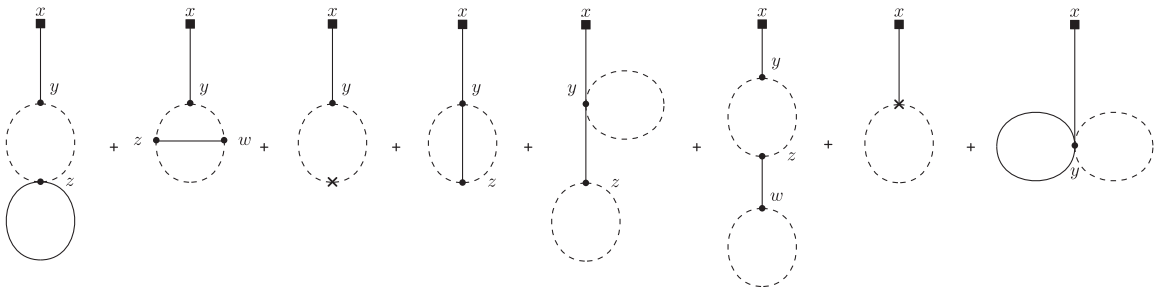

FIG. 4. Contributions to the expectation value of $A(x)$ at 2-loop order.

$$\boxed{\langle\Omega|A(x)|\Omega\rangle = \frac{\lambda H^2}{16\pi^2}\left[\ln(a) - \frac{1}{3} + \frac{1}{3a^3}\right] + \mathcal{O}(\lambda^3)}. \quad (17)$$

The 2-loop contributions are shown in Fig. 4. The first seven diagrams (which we label A_{2a} through A_{2g}) were calculated in [15]. We need only include a relative factor of $\frac{3}{2}$ for each 4-point coupling to express their final contributions, at leading logarithm order, as multiples of the factor $S \equiv \lambda^3 H^4 \ln^2(a)/2^{10}\pi^4$,

$$A_{2a} \to -3 \cdot S, \qquad A_{2b} \to +8 \cdot S, \qquad A_{2c} \to 0 \cdot S,$$
$$A_{2d} \to -6 \cdot S, \quad (18)$$

$$A_{2e} \to +\frac{3}{2} \cdot S, \qquad A_{2f} \to -2 \cdot S, \qquad A_{2g} \to 0 \cdot S. \quad (19)$$

Only the last diagram, A_{2h}, is really new. It has a symmetry factor of $\frac{1}{4}$, and its initial expression is

$$A_{2h} = \frac{-i}{4} \cdot \frac{3\lambda^3}{8} \cdot \int d^D y \sqrt{-g(y)} g^{\mu\nu}(y) \cdot i\Delta(x;y) \cdot i\Delta(y;y) \cdot \partial^z_\mu \partial^y_\nu i\Delta(y;z)\Big|_{y=z}. \quad (20)$$

The two coincidence limits can be read from (15) and (16) to give

$$A_{2h} = \frac{3i\lambda^3}{2^5}(D-1)kH^2 I_2, \quad (21)$$

where I_2, and its leading logarithm result, was given in [18],

$$I_2 \equiv \int d^D y \sqrt{-g(y)} i\Delta(x;y) i\Delta(y;y) \to -\frac{i}{24\pi^2} \times \ln^2(a). \quad (22)$$

This is finite and does not require renormalization, so we can set $D = 4$,

$$A_{2h} \to \frac{3}{2} \cdot S. \quad (23)$$

Adding this to the leading logarithm results for the first seven diagrams gives

$$A_{2a} \to -3 \cdot S, \qquad A_{2b} \to +8 \cdot S, \qquad A_{2c} \to 0 \cdot S,$$
$$A_{2d} \to -6 \cdot S, \quad (24)$$

$$A_{2e} \to +\frac{3}{2} \cdot S, \qquad A_{2f} \to -2 \cdot S, \qquad A_{2g} \to 0 \cdot S,$$
$$A_{2h} \to +\frac{3}{2} \cdot S. \quad (25)$$

At leading logarithm order the eight diagrams of Fig. 4 sum to zero, so our result for the expectation value of A is

$$\boxed{\langle\Omega|A(x)|\Omega\rangle = \frac{\lambda H^2 \ln(a)}{16\pi^2}[1+0] + \mathcal{O}(\lambda^4)}. \quad (26)$$

B. The 1-loop self-masses

We now move on to the 1-loop self-masses. Absorbing the divergences of these reveals curvature-dependent field strength renormalizations Z_A and Z_B from the terms proportional to C_{2A^2} and C_{2B^2} in expression (10). These give the γ functions that will be used in the renormalization group (RG) analysis of Sec. IV.

The 1-loop contributions to $-iM^2_A(x;x')$ are shown in Fig. 5. The first diagram is unchanged from the old model, and the second diagram is just $\frac{3}{2}$ times the previous result [5],

$$-iM^2_{A_3}(x;x') = \frac{(-i\lambda)^2}{2}\Big\{\frac{1}{4}\mathcal{D}\mathcal{D}'[i\Delta(x;x')]^2 - \frac{1}{2}\mathcal{D}[i\Delta(x;x)i\delta^D(x-x')] - kHa^{D-1}\partial_0 i\delta^D(x-x')\Big\}, \quad (27)$$

FIG. 5. The 1-loop contributions to the A self-mass $-iM^2_A(x;x')$.

$$-iM^2_{A_4}(x;x') = -\frac{i3\lambda^2}{8}\delta^D(x-x')\times -(D-1)kH^2a^D. \quad (28)$$

The counterterm is i times the second variation of (10),

$$-iM^2_{Ac}(x;x') = -C_{1A^2}\mathcal{D}\mathcal{D}'\left[\frac{i\delta^D(x-x')}{(aa')^{\frac{D}{2}}}\right] + C_{2A^2}\partial^\mu[Ra^{D-2}\partial_\mu i\delta^D(x-x')]. \quad (29)$$

Because only (27) diverges in dimensional regularization, and this diagram is identical to the old model, so too are the coefficients C_{A_1} and C_{A_2},

$$C_{1A^2} = -\frac{\lambda^2\mu^{D-4}}{32\pi^{\frac{D}{2}}}\frac{\Gamma\left(\frac{D}{2}-1\right)}{2(D-3)(D-4)},$$
$$C_{2A^2} = \frac{\lambda^2\mu^{D-4}}{4(4\pi)^{\frac{D}{2}}}\frac{\Gamma(D-1)}{\Gamma\left(\frac{D}{2}\right)}\frac{\pi\cot\left(\frac{D\pi}{2}\right)}{D(D-1)}. \quad (30)$$

We move to the B self-mass, whose 1-loop contributions are shown in Fig. 6. As before, the 3-point diagram is unchanged from the old model, and the 4-point diagram is just the result from the old model times $\frac{3}{2}$,

$$-iM^2_{B_3} = \frac{(i\lambda)^2}{2}\mathcal{D}\mathcal{D}'[i\Delta(x;x')]^2 - (i\lambda)^2\partial^\mu\partial'^\rho[(aa')^{D-2}\partial_\mu i\Delta(x;x')\partial'_\rho i\Delta(x;x')], \quad (31)$$

$$-iM^2_{B_4} = -\frac{3\lambda^2 k\pi\cot\left(\frac{D\pi}{2}\right)\mathcal{D}}{8}[i\delta^D(x-x')] + \frac{3\lambda^2H^2\partial^\mu}{32\pi^2}[\ln(a)a^2\partial_\mu i\delta^4(x-x')] + \mathcal{O}(D-4). \quad (32)$$

The counterterm is i times the second variation of (10) with respect to B,

$$-iM^2_{B_c}(x;x') = -C_{1B^2}\mathcal{D}\mathcal{D}'\left[\frac{i\delta^D(x-x')}{(aa')^{\frac{D}{2}}}\right] + C_{2B^2}\partial^\mu[Ra^{D-2}\partial_\mu i\delta^D(x-x')]. \quad (33)$$

Multiplying the divergences from (32) by $\frac{3}{2}$ and combining with those from (31) gives

$$C_{1B^2} = -\frac{\lambda^2\mu^{D-4}}{16\pi^{\frac{D}{2}}}\frac{\Gamma\left(\frac{D}{2}-1\right)}{2(D-3)(D-4)}, \quad (34)$$

$$C_{2B^2} = \frac{3\lambda^2\mu^{D-4}}{8(4\pi)^{\frac{D}{2}}}\frac{\Gamma(D-1)}{\Gamma\left(\frac{D}{2}\right)}\frac{\pi\cot\left(\frac{D\pi}{2}\right)}{D(D-1)} - \frac{\lambda^2\mu^{D-4}}{32\pi^{\frac{D}{2}}}\frac{\Gamma\left(\frac{D}{2}-1\right)}{2(D-3)(D-4)}\frac{D-2}{D-1}. \quad (35)$$

C. The 1-loop vertex function

In this subsection we first isolate the primitive divergences of the 3-point vertex $-iV(x;y;z)$ at 1-loop order. These divergences are removed by the counterterm (11), which determines the coefficients C_{1AB^2}, C_{2AB^2}, C_{3AB^2}, and C_{4AB^2}. We regard the C_{4AB^2} counterterm as a curvature-dependent renormalization of the bare 3-point coupling and infer the corresponding beta function as

$$\delta\lambda = C_{4AB^2}\times R + O(\lambda^5) \Rightarrow \beta \equiv \frac{\partial\delta\lambda}{\partial\ln(\mu)}. \quad (36)$$

The tree order vertex can be inferred from the Feynman rules,

$$-iV_0(x;y;z) = -i\lambda\sqrt{-g(x)}g^{\mu\nu}_x\partial_\mu\delta^D(x-y)\partial_\nu\delta^D(x-z). \quad (37)$$

The various 1-loop contributions are shown in Fig. 7. Because the leftmost diagram involves only 3-point couplings, it is unchanged from the old model [16],

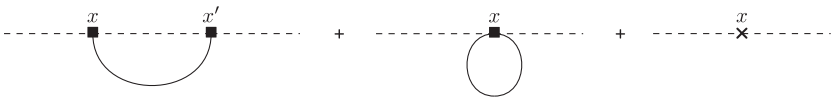

FIG. 6. The 1-loop contributions to the B self-mass $-iM^2_B(x;x')$.

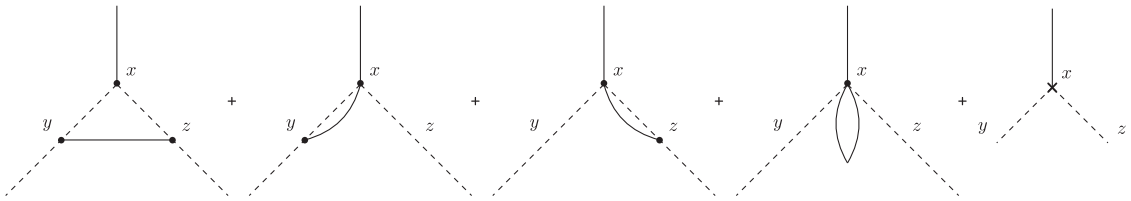

FIG. 7. The 1-loop contributions to the ABB vertex $-iV(x;y;z)$.

$$-iV_{1a}(x;y;z) = \frac{i\lambda^3}{2}\mathcal{D}_x\partial_\sigma^y\partial_\beta^z\Big\{\sqrt{-g_y}g_y^{\rho\sigma}\partial_\rho^y i\Delta(x;y)\sqrt{-g_z}g_z^{\alpha\beta}\partial_\alpha^z i\Delta(x;z)i\Delta(y;z)\Big\}$$
$$+\frac{\lambda^3}{4}\mathcal{D}_y\mathcal{D}_z\Big\{\Big[i\Delta(y;z)\Big]^2\Big[\delta^D(x-y)+\delta^D(x-z)\Big]\Big\}$$
$$-\frac{\lambda^3}{2}\partial_\sigma^y\partial_\beta^z\Big\{\sqrt{-g_y}g_y^{\rho\sigma}\partial_\rho^y i\Delta(y;z)\sqrt{-g_z}g_z^{\alpha\beta}\partial_\alpha^z i\Delta(y;z)\Big[\delta^D(x-y)+\delta^D(x-z)\Big]\Big\}. \tag{38}$$

The second and third diagrams involve a single 4-point coupling and are therefore $\frac{3}{2}$ times the results of the old model [16],

$$-iV_{1b}(x;y;z) = \frac{3\lambda^3}{8}\mathcal{D}_y\Big\{\sqrt{-g_x}g_x^{\mu\nu}\partial_\mu^x\Big[i\Delta(x;y)\Big]^2\partial_\nu\delta^D(x-z)\Big\}+\frac{3\lambda^3}{4}\partial_\nu^z\partial_\beta^y\Big\{\sqrt{-g_z}g_z^{\mu\nu}\partial_\mu^z i\Delta(z;y)$$
$$\times\sqrt{-g_y}g_y^{\alpha\beta}\partial_\alpha^y i\Delta(z;y)\delta^D(x-z)\Big\}, \tag{39}$$

$$-iV_{1c}(x;y;z) = \frac{3\lambda^3}{8}\mathcal{D}_z\Big\{\sqrt{-g_x}g_x^{\mu\nu}\partial_\mu^x[i\Delta(x;z)]^2\partial_\nu\delta^D(x-y)\Big\}+\frac{3\lambda^3}{4}\partial_\sigma^y\partial_\beta^z\Big\{\sqrt{-g_y}g_y^{\rho\sigma}\partial_\rho^y i\Delta(y;z)$$
$$\times\sqrt{-g_z}g_z^{\alpha\beta}\partial_\alpha^z i\Delta(y;z)\delta^D(x-y)\Big\}. \tag{40}$$

Before considering the fourth diagram, we combine and reduce expressions (38)–(40). Because the last two differ from the old model, the reduction is more complicated. Adding all three terms and performing some judicious partial integrations gives

$$-iV_{1abc} = \frac{i\lambda^3}{2}\mathcal{D}_x\partial_y^\rho\partial_z^\alpha\Big\{(a_ya_z)^{D-2}i\Delta(y;z)\partial_\rho^y i\Delta(x;y)\partial_\alpha^z i\Delta(x;z)\Big\}+\frac{3\lambda^3}{8}\mathcal{D}_y\partial_z^\alpha\Big\{a_z^{D-2}\Big[i\Delta(y;z)\Big]^2\partial_\alpha^z\delta^D(x-z)\Big\}$$
$$+\frac{3\lambda^3}{8}\mathcal{D}_z\partial_y^\alpha\Big\{a_y^{D-2}\Big[i\Delta(y;z)\Big]^2\partial_\alpha^y\delta^D(x-y)\Big\}-\frac{\lambda^3}{8}\mathcal{D}_y\mathcal{D}_z\Big\{\Big[i\Delta(y;z)\Big]^2\Big[\delta^D(x-y)+\delta^D(x-z)\Big]\Big\}$$
$$+\frac{\lambda^3}{4}\partial_y^\rho\partial_z^\alpha\Big\{(a_ya_z)^{D-2}\partial_\rho^y i\Delta(y;z)\partial_\alpha^z i\Delta(y;z)\Big[\delta^D(x-y)+\delta^D(x-z)\Big]\Big\}. \tag{41}$$

After considerable manipulations explained in the Appendix A expression, the divergent part of (41) can be brought to the form

$$-iV_{1abc}(x;y;z)\to-\frac{i\lambda^3\Gamma\Big(\frac{D}{2}+1\Big)\mu^{D-4}H^2a_x^2}{32\pi^{\frac{D}{2}}(D-3)(D-4)}\partial^\mu\delta^D(x-y)\partial_\mu\delta^D(x-z)-i\tilde{V}(x;y;z), \tag{42}$$

where $-i\tilde{V}(x;y;z)$ consists of higher derivative divergences,

$$-i\tilde{V}(x;y;z) = \frac{i\lambda^3\mu^{D-4}}{16\pi^{\frac{D}{2}}}\frac{\Gamma\left(\frac{D}{2}-1\right)}{D(D-3)(D-4)}\mathcal{D}_x\left[\frac{\partial_\mu\delta^D(x-y)\partial^\mu\delta^D(x-z)}{a_x^{D-2}}\right]$$
$$+\frac{5i\lambda^3\mu^{D-4}\Gamma\left(\frac{D}{2}-1\right)}{128\pi^{\frac{D}{2}}(D-3)(D-4)}\left\{\mathcal{D}_y\partial_x^\mu\left[\frac{\delta^D(x-y)\partial_\mu\delta^D(x-z)}{a_x^{D-2}}\right]+\mathcal{D}_z\partial_x^\mu\left[\frac{\partial_\mu\delta^D(x-y)\cdot\delta^D(x-z)}{a_x^{D-2}}\right]\right\}$$
$$-\frac{\lambda^3\Gamma\left(\frac{D}{2}-1\right)\mu^{D-4}}{64\pi^{\frac{D}{2}}(D-3)(D-4)}\mathcal{D}_y\mathcal{D}_z\left[\frac{i\delta^D(x-z)\delta^D(x-y)}{a_x^{2D-4}}\right]. \tag{43}$$

We call the new diagram $-iV_{1d}(x;y;z)$, and its contribution is

$$-iV_{1d} = -i\frac{3\lambda^3}{16}\sqrt{-g(x)}g^{\mu\nu}(x)\partial_\mu\delta^D(x-y)$$
$$\times\,\partial_\nu\delta^D(x-z)\cdot i\Delta(x;x). \tag{44}$$

This is just the bare vertex (37) times the simple factor $\frac{3\lambda^2}{16}i\Delta(x;x)$. Recall that the coincident propagator is given in Eq. (15),

$$-iV_{1d} = -i\frac{3\lambda^3}{16}a_x^{D-2}\partial^\mu\delta^D(x-y)$$
$$\times\,\partial_\mu\delta^D(x-z)k\left[-\pi\cot\left(\frac{D\pi}{2}\right)+2\,\ln(a)\right] \tag{45}$$
$$=-i\frac{3\lambda^3 k}{16}\times-\pi\,\cot\left(\frac{D\pi}{2}\right)$$
$$\times\,a_x^2\partial^\mu\delta^D(x-y)\partial_\mu\delta^D(x-z)+O(D-4). \tag{46}$$

Adding the primitive divergences from (42) to this gives

$$-iV_{1\text{pdiv}}(x;y;z) = -i\frac{\lambda^3H^2a_x^2}{8}\partial^\mu\delta^D(x-y)\partial_\mu\delta^D(x-z)$$
$$\times\left[\frac{3k}{2H^2}\times-\pi\cot\left(\frac{D\pi}{2}\right)+\frac{\mu^{D-4}\Gamma(\frac{D}{2}+1)}{4\pi^{\frac{D}{2}}(D-3)(D-4)}\right]-i\tilde{V}(x;y;z). \tag{47}$$

The primitive divergences (47) are absorbed by the third variation of (11),

$$\frac{i\delta^3S_{AB^2}[A,B]}{\delta A(x)\delta B(y)\delta B(z)} = -iC_{1AB^2}\mathcal{D}_x\left[\frac{\partial^\mu\delta^D(x-y)\partial_\mu\delta^D(x-z)}{a_x^2}\right]+iC_{2AB^2}\mathcal{D}_y\partial_x^\mu\left[\frac{\delta^D(x-y)\partial_\mu\delta^D(x-z)}{a_x^2}\right]$$
$$+iC_{2AB^2}\mathcal{D}_z\partial_x^\mu\left[\frac{\partial_\mu\delta^D(x-y)\times\delta^D(x-z)}{a_x^2}\right]-iC_{3AB^2}\mathcal{D}_y\mathcal{D}_z\left[\frac{\delta^D(x-y)\delta^D(x-z)}{a_x^D}\right]$$
$$-iC_{4AB^2}Ra_x^2\partial^\mu\delta^D(x-y)\partial_\mu\delta^D(x-z). \tag{48}$$

Adding (48) to (47) and demanding regularity as $D\to4$ implies

$$C_{1AB^2} = \frac{\lambda^3\mu^{D-4}\Gamma\left(\frac{D}{2}-1\right)}{16\pi^{\frac{D}{2}}D(D-3)(D-4)}, \tag{49}$$

$$C_{2AB^2} = -\frac{5\lambda^3\mu^{D-4}\Gamma\left(\frac{D}{2}-1\right)}{128\pi^{\frac{D}{2}}(D-3)(D-4)}, \tag{50}$$

$$C_{3AB^2} = -\frac{\lambda^3\mu^{D-4}\Gamma\left(\frac{D}{2}-1\right)}{64\pi^{\frac{D}{2}}(D-3)(D-4)}, \tag{51}$$

$$C_{4AB^2} = \frac{\lambda^3\mu^{D-4}}{32\pi^{\frac{D}{2}}D(D-1)}\left[\frac{3\pi\cot\left(\frac{D\pi}{2}\right)\Gamma(D-1)}{8\Gamma(\frac{D}{2})}-\frac{\Gamma\left(\frac{D}{2}+1\right)}{(D-3)(D-4)}\right]. \tag{52}$$

Because we have suppressed the finite contributions the renormalized result will not be given, but let us take note of the fact that logarithms of μ come in the form $\ln(\frac{\mu a}{H})$. We can regard $C_{4AB^2} \times R = \delta\lambda$ as a curvature-dependent renormalization. The associated 1-loop beta function (36) is

$$\boxed{\beta = \frac{\partial \delta\lambda}{\partial \ln(\mu)} = -\frac{\lambda^3 H^2}{64\pi^2} + O(\lambda^5)}. \tag{53}$$

IV. SUMMING THE LOGARITHMS

Here we demonstrate that the results of the previous section for the new model (8) can be explained using the same combination of Starobinsky's stochastic formalism and the renormalization group that worked for the old model (5). We begin by deriving the curvature-dependent effective potential and showing that it explains the evolution of the background. We next apply our explicit results for the 1-loop counterterms to work out the curvature-dependent renormalization group corrections.

A. Curvature-dependent effective potential

The shift symmetry of the field $B(x)$ evident in (8) prevents it from developing an effective potential. However, $A(x)$ does acquire one from integrating out the differentiated B fields from the A field equation in the presence of a constant $A(x) = A_0$ background,

$$\frac{\delta S[A,B]}{\delta A(x)} = \partial_\mu\Big[\sqrt{-g}g^{\mu\nu}\partial_\nu A\Big] - \frac{\lambda}{2}\left(1+\frac{\lambda}{4}A\right)^3 \times \partial_\mu B \partial_\nu B g^{\mu\nu}\sqrt{-g} = 0. \tag{54}$$

One can see from the Lagrangian (8) that a constant $A(x) = A_0$ background just renormalizes the B field strength,

$$\langle\Omega|T[B(x)B(x')]|\Omega\rangle_{A=A_0} = \frac{i\Delta(x;x')}{(1+\frac{\lambda}{4}A_0)^4}. \tag{55}$$

Hence the A equation can be recognized as that of a scalar potential model,

$$\frac{\delta S[A,B]}{\delta A(x)} \to \partial_\mu\Big[\sqrt{-g}g^{\mu\nu}\partial_\nu A\Big] - \frac{\lambda}{2}\left(1+\frac{\lambda}{4}A\right)^3 \times \frac{\sqrt{-g}g^{\mu\nu}\partial_\mu\partial'_\nu i\Delta(x;x')|_{x'=x}}{\left(1+\frac{\lambda}{4}A\right)^4} \tag{56}$$

$$= \partial_\mu\Big[\sqrt{-g}g^{\mu\nu}\partial_\nu A\Big] + \frac{\left(\frac{D-1}{2}\right)\lambda k H^2\sqrt{-g}}{1+\frac{\lambda}{4}A} \equiv \partial_\mu\Big[\sqrt{-g}g^{\mu\nu}\partial_\nu A\Big] - V'_{\rm eff}(A)\sqrt{-g}. \tag{57}$$

Note that we have employed expression (16) to evaluate the coincidence limit of the doubly differentiated propagator. This is free of divergences, so we can set $D = 4$ to find

$$V'_{\rm eff}(A) = -\frac{3\lambda H^4}{16\pi^2}\left(1+\frac{\lambda}{4}A\right)^{-1} \Rightarrow V_{\rm eff}(A) = -\frac{3H^4}{4\pi^2}\ln\left(1+\frac{\lambda}{4}A\right). \tag{58}$$

We see that the new model's curvature-dependent effective potential (58) is almost the same as the old model's result of $-\frac{3H^4}{8\pi^2}\ln(1+\frac{\lambda}{2}A)$ [15].

Starobinsky long ago showed how to sum the leading logarithms of a scalar potential model like (57) [13,14]. The leading logarithms contained in correlators of the quantum field $A(t,\vec{x})$ turn out to agree, to all orders [9], with those of stochastic random field $\mathcal{A}(t,\vec{x})$ which obeys the Langevin equation

$$3H[\dot{\mathcal{A}} - \dot{\mathcal{A}}_0] = V'_{\rm eff}(\mathcal{A}). \tag{59}$$

The "stochastic jitter" in this equation is supplied by the time derivative of the infrared-truncated, free field expansion of $A(t,\vec{x})$,

$$\mathcal{A}_0(t,\vec{x}) \equiv \int_H^{aH}\frac{d^3k}{(2\pi)^3}\frac{H}{\sqrt{2k^3}}\Big\{\alpha(\vec{k})e^{i\vec{k}\cdot\vec{x}} + \alpha^\dagger(\vec{k})e^{-i\vec{k}\cdot\vec{x}}\Big\}, \quad [\alpha(\vec{k}),\alpha^\dagger(\vec{k}')] = (2\pi)^3\delta^3(\vec{k}-\vec{k}'). \tag{60}$$

If we turn off the stochastic jitter, then Eq. (59) is simple to solve, adopting the initial condition $\mathcal{A}(0,\vec{x}) = 0$ and noting that $\ln(a) = Ht$,

$$\mathcal{A}(t,\vec{x})|_{\mathcal{A}_0=0} = \frac{4}{\lambda}\left[\sqrt{1+\frac{\lambda^2H^2\ln(a)}{32\pi^2}} - 1\right] = \frac{\lambda H^2\ln(a)}{16\pi^2} - \frac{\lambda^3H^4\ln^2(a)}{2^{11}\pi^4} + O(\lambda^5). \tag{61}$$

Because it is easier to fluctuate down the potential than up, we expect that the effect of adding stochastic jitter is to accelerate the evolution of $\mathcal{A}$ down its potential. Solving (59) perturbatively gives

$$\mathcal{A} = \mathcal{A}_0 + \frac{\lambda H^2\ln(a)}{16\pi^2} - \frac{\lambda^2H^3}{2^6\pi^2}\int_0^t dt'\mathcal{A}_0(t',\vec{x}) - \frac{\lambda^3H^4\ln^2(a)}{2^{11}\pi^4} + \frac{\lambda^3H^3}{2^8\pi^2}\int_0^t dt'\mathcal{A}_0^2(t',\vec{x}) + O(\lambda^4). \tag{62}$$

By taking the expectation value of the previous equation, and using the mode sum (60) to conclude,

$$\langle\Omega|\mathcal{A}_0(t,\vec{x})|\Omega\rangle = 0, \qquad \langle\Omega|\mathcal{A}_0^2(t,\vec{x})|\Omega\rangle = \frac{H^2\,\ln(a)}{4\pi^2}, \tag{63}$$

we find

$$\langle\Omega|\mathcal{A}(t,\vec{x})|\Omega\rangle = \frac{\lambda H^2\,\ln(a)}{16\pi^2} + O(\lambda^5). \tag{64}$$

This is exactly the result (26) we got by explicit computation, which is impressive confirmation of the stochastic prediction.

B. Curvature-dependent renormalization group

In a theory with derivative interactions not all of the large logarithms derive from stochastic effects. Some of them arise instead from the incomplete cancellation between primitive divergences—which have no D-dependent powers of the scale factor—and counterterms—which inherit a a^D from the measure factor $\sqrt{-g}$,

$$\left(\frac{H^{D-4}}{D-4}\right) - \left(\frac{\mu^{D-4}a^{D-4}}{D-4}\right) = -\ln\left(\frac{\mu a}{H}\right) + O(D-4). \tag{65}$$

These logarithms can be recovered using the renormalization group, which follows factors of $\ln(\mu)$. Because we are only interested in cases where the factors of $\ln(a)$ are not suppressed by inverse powers of the scale factor, the counterterms of concern are those that can be viewed as curvature-dependent renormalizations of bare parameters [15]. Of the four counterterms (11) required to renormalize the vertex function at 1-loop order we have already seen that the contribution proportional to C_{4AB^2} can be viewed as a curvature-dependent renormalization of the bare vertex, and we used this to compute the associated beta function (36). Of the four counterterms (10) required to renormalize the 1-loop self-masses it is the contributions proportional to C_{2A^2} and C_{2B^2} that can be regarded as curvature-dependent field strength renormalizations,

$$Z_A \equiv 1 + C_{2A^2} \times R + O(\lambda^4),$$
$$Z_B \equiv 1 + C_{2B^2} \times R + O(\lambda^4). \tag{66}$$

Our explicit results (30) and (35) give the associated gamma functions,

$$\boxed{\gamma_A \equiv \frac{\partial\,\ln(Z_A)}{\partial\,\ln(\mu^2)} = \frac{\lambda^2 H^2}{32\pi^2} + O(\lambda^4), \qquad \gamma_B \equiv \frac{\partial\,\ln(Z_B)}{\partial\,\ln(\mu^2)} = -\frac{\lambda^2 H^2}{64\pi^2} + O(\lambda^4).} \tag{67}$$

We are ready to investigate the Callan-Symanzik equations for the n-point Green functions $G_n(x_1;x_2;\ldots;x_n;\lambda;\mu)$ of the field A,[2]

$$\left[\mu\frac{\partial}{\partial\mu} + \beta\frac{\partial}{\partial\lambda} + n\gamma_A\right] G_n(x_1;x_2;\ldots;x_n;\lambda;\mu) = 0. \tag{68}$$

This equation can be solved using the method of characteristics. We first find a running coupling constant $\bar{\lambda}(\mu)$ which obeys the differential equation and initial condition,

$$\mu\frac{d\bar{\lambda}}{d\mu} = -\beta(\bar{\lambda}(\mu)), \qquad \bar{\lambda}(\mu_0) = \lambda \Rightarrow \beta(\lambda)\frac{\partial\bar{\lambda}}{\partial\lambda} = \beta(\bar{\lambda}). \tag{69}$$

We can then write the solution as

$$G_n(x_1;x_2;\ldots;x_n;\lambda;\mu) = G_n(x_1;x_2;\ldots;x_n;\bar{\lambda}(\mu);\mu_0) \times \exp\left[-n\int_{\mu_0}^{\mu}\frac{d\mu'}{\mu'}\gamma(\bar{\lambda}(\mu'))\right]. \tag{70}$$

[2]The 1PI n-point functions obey a similar equation with the last term replaced by $-n\gamma_A$.

Inserting the β function (53) into (69), and ignoring higher loop corrections yields

$$\bar{\lambda}(\mu) = \frac{\lambda}{\sqrt{1 - \frac{\lambda^2 H^2}{32\pi^2}\,\ln\left(\frac{\mu}{\mu_0}\right)}}. \tag{71}$$

Substituting (71) and (67) into (70), and again ignoring higher loop corrections, gives

$$G_n(x_1;x_2;\ldots x_n;\lambda;\mu) = G_n(x_1;x_2;\ldots;x_n;\bar{\lambda}(\mu);\mu_0) \times \left[1 - \frac{\lambda^2 H^2}{32\pi^2}\,\ln\left(\frac{\mu}{\mu_0}\right)\right]^n. \tag{72}$$

Similar results could be derived for Green's functions, which also, or even exclusively, involve the field $B(x)$.

Having a negative beta function traditionally means that the theory runs toward weak coupling in the ultraviolet because logarithms of the scale μ are associated with inverse factors of some characteristic momentum in the process. In cosmology we are interested in how things behave at *late times*, and we note from expression (65) that the scale μ is associated with the scale factor $a(t)$ in the form $\ln[\mu a/H]$. It should therefore be that having a negative

beta function means the theory evolves toward strong coupling at late times.

V. CONCLUSION

In this work, we examined a nontrivial nonlinear sigma model (defined in Sec. II) whose loop corrections on the de Sitter background show the same large logarithms as have been reported from inflationary gravitons [3–8]. Previous work [15,16] on nonlinear sigma models which can be reduced to free theories has shown that these large logarithms can be resummed by combining a variant of Starobinsky's stochastic formalism [13,14]—based on curvature-dependent effective potentials—with a variant of the renormalization group—based on the subset of counterterms that can be viewed as curvature-dependent renormalizations of bare parameters. Our analysis confirms that these techniques continue to apply for models whose S-matrix is nontrivial. In Sec. III A, we explicitly computed the evolution of the background (26) at 1-loop and 2-loop orders. In Sec. IV A we showed that the resummation techniques correctly predict these results.

One significant difference associated with a nontrivial S-matrix is that the beta function does not vanish. The 1-loop beta function (53) was derived in Sec. III C. The 1-loop gamma functions (67) were derived in Sec. III B, and combined with the beta function in Sec. IV B, to solve the Callan-Symanzik equation for n-point Green's functions (72). Because the beta function (53) is negative, the running coupling constant $\bar{\lambda}(\mu)$ grows with the scale μ as shown in Eq. (71). From (65) we see that logarithms of μ are associated with the scale factor $a(t)$ in the form $\ln[\mu a(t)/H]$. This implies that the model becomes strongly coupled at late times.

An interesting higher loop phenomenon is that there can be mixing of large stochastic logarithms with large logarithms from the renormalization group. We speculate that the correct way to include these is to use the renormalization group to improve the curvature-dependent effective potential and then use that, without any extra RG corrections. From (67) we observe that, because $\gamma_A \sim \lambda^2$, an RG improvement to the effective potential (58) will include lowest order corrections of the form $\lambda^3 A$. Those would not engender any changes in the background evolution at leading logarithm order.

We should comment on how this work can be extended to slow-roll inflation models, in particular to ultra-slow-roll inflation in which a nearly flat region of the potential causes the scalar to almost stop rolling [26]. One must be clear that neither of the nonlinear sigma model scalars $A(x)$ and $B(x)$ serves as the inflaton; they are just spectators to inflation driven by some other scalar field.[3] In this case exact calculations are no longer possible because we lack the propagators for a general inflationary background. However, the great thing about the resummation technique described in Sec. IV is that it can be implemented on a general inflationary background. The stochastic formalism described in Sec. IV A relies on a curvature-dependent effective potential whose effective force (56) derives from the coincidence limit of the doubly differentiated free scalar propagator $\partial_\mu \partial'_\nu i\Delta(x;x')$ in the appropriate background. Although we do not have exact expressions for this quantity, very good analytic approximations have been developed [17], and one can use them to solve the resulting Langevin equation (59) numerically for any cosmological background which has experienced primordial inflation [18]. If the analytic approximations should happen to become unreliable for a particular expansion history, they can easily be improved [27]. The situation for the curvature-dependent renormalization group described in Sec. IV B is even better because the coefficients of the counterterms are universal, independent of the background geometry.

The infrared modes that engender the large logarithms which we have studied are fascinating, but experience with gravity [28–32] shows that one must employ a resummation technique which goes beyond linearized order in order to understand what happens when perturbation theory breaks down. Although our 1-loop and 2-loop results are obviously perturbative, we emphasize that they were made merely to check the validity of the resummation technique of Sec. IV, which is fully nonperturbative. One can see that the technique includes nonlinear effects from the form (58) of the curvature-dependent effective potential. Note also that its field dependence of $\ln(1+\frac{\lambda}{4}A)$ applies to *any* cosmological background; only the multiplicative coefficient of $-\frac{3H^4}{4\pi^2}$ changes when the geometry is no longer de Sitter. The solution (61) that results from ignoring stochastic jitter is similarly nonperturbative—and it should generally be true that jitter merely serves to accelerate the rate at which the A background rolls down the effective potential. Finally, the renormalization group formalism sums logarithms that result from renormalization (65) to all orders in perturbation theory.

ACKNOWLEDGMENTS

This work was partially supported by NSF Grant No. PHY-2207514 and by DOE Grant No. DE-SC0022148 and by the Institute for Fundamental Theory at the University of Florida.

APPENDIX A: REDUCTION OF THE 1-LOOP VERTEX FUNCTION

The aim of this appendix is to reduce the last line of Eq. (41) for $-iV_{1abc}(x;y;z)$,

[3]To make A or B the inflaton would require the introduction of a potential for them, which is a very substantial modification of the model.

$$I(x;y;z) \equiv \frac{\lambda^3}{4} \partial_y^\rho \partial_z^\alpha \Big\{ (a_y a_z)^{D-2} \partial_\rho^y i\Delta(y;z) \partial_\alpha^z i\Delta(y;z) \Big[\delta^D(x-y) + \delta^D(x-z) \Big] \Big\}. \tag{A1}$$

Note that $\partial_\rho^y i\Delta(y;z)\partial_\alpha^z i\Delta(y;z)$ is quadratically divergent, so extracting just the divergent part of $I(x;y;z)$ requires only the two terms given on the first line of expansion (14) for each propagator,

$$\partial_\rho^y i\Delta(y;z) = -\frac{\Gamma\left(\frac{D}{2}\right)}{2\pi^{\frac{D}{2}}(a_y a_z)^{\frac{D}{2}-1}} \left[\frac{(y-z)_\rho}{(y-z)^D} + \frac{a_y H \delta^0_\rho}{2(y-z)^{D-2}} + \frac{D a_y a_z H^2 (y-z)_\rho}{8(y-z)^{D-2}} + \cdots \right], \tag{A2}$$

$$\partial_\alpha^z i\Delta(y;z) = -\frac{\Gamma\left(\frac{D}{2}\right)}{2\pi^{\frac{D}{2}}(a_y a_z)^{\frac{D}{2}-1}} \left[-\frac{(y-z)_\alpha}{(y-z)^D} + \frac{a_z H \delta^0_\alpha}{2(y-z)^{D-2}} - \frac{D a_y a_z H^2 (y-z)_\alpha}{8(y-z)^{D-2}} + \cdots \right]. \tag{A3}$$

Multiplying (A2) and (A3), and retaining only potentially divergent terms yields

$$\begin{aligned} \partial_\rho^y i\Delta(y;z) \times \partial_\alpha^z i\Delta(y;z) = \frac{\Gamma^2\left(\frac{D}{2}\right)}{4\pi^D (a_y a_z)^{D-2}} \Bigg\{ & -\frac{(y-z)_\rho (y-z)_\alpha}{(y-z)^{2D}} + \frac{a_z H \delta^0_\alpha (y-z)_\rho}{2(y-z)^{2D-2}} \\ & - \frac{a_y H \delta^0_\rho (y-z)_\alpha}{2(y-z)^{2D-2}} + \frac{a_y a_z H^2 \delta^0_\rho \delta^0_\alpha}{4(y-z)^{2D-4}} - \frac{D a_y a_z H^2 (y-z)_\rho (y-z)_\alpha}{4(y-z)^{2D-2}} + \cdots \Bigg\}. \end{aligned} \tag{A4}$$

The first four terms and the last term inside the curly bracket in (A4) require separate reductions which we give below.

We first extract two derivatives from the first four terms of expression (A4),

$$\begin{aligned} & \frac{\Gamma^2\left(\frac{D}{2}\right)}{16\pi^D (a_y a_z)^{D-2}} \left\{ -\frac{(y-z)_\rho (y-z)_\alpha}{(y-z)^{2D}} + \frac{a_z H \delta^0_\alpha (y-z)_\rho}{2(y-z)^{2D-2}} - \frac{a_y H \delta^0_\rho (y-z)_\alpha}{2(y-z)^{2D-2}} + \frac{a_y a_z H^2 \delta^0_\rho \delta^0_\alpha}{4(y-z)^{2D-4}} \right\} \\ & = \frac{\Gamma^2\left(\frac{D}{2}-1\right)}{64\pi^D} \left\{ \partial_\rho^y \partial_\alpha^z \left[\frac{1}{(a_y a_z)^{D-2}(y-z)^{2D-4}} \right] + \frac{[\partial_\rho^y \partial_\alpha^y - \eta_{\rho\alpha}\partial_y^2]}{(D-1)(a_y a_z)^{D-2}} \left[\frac{1}{(y-z)^{2D-4}} \right] \right\}. \end{aligned} \tag{A5}$$

The denominator $(y-z)^{2D-4}$ is logarithmically divergent so we can extract a local divergence from it by adding the flat space propagator equation [24,25]

$$\frac{1}{(y-z)^{2D-4}} = \frac{\mu^{D-4}}{2(D-3)(D-4)} \frac{4\pi^{\frac{D}{2}} i\delta^D(y-z)}{\Gamma\left(\frac{D}{2}-1\right)} - \frac{\partial_y^2}{4} \left[\frac{\ln[\mu^2 (y-z)^2]}{(y-z)^2} \right] + O(D-4). \tag{A6}$$

Substituting (A6) in (A5), and retaining only the divergences, reduces the first four terms of expression (A4) to

$$\begin{aligned} & \frac{\Gamma^2\left(\frac{D}{2}\right)}{16\pi^D (a_y a_z)^{D-2}} \left\{ -\frac{(y-z)_\rho (y-z)_\alpha}{(y-z)^{2D}} + \frac{a_z H \delta^0_\alpha (y-z)_\rho}{2(y-z)^{2D-2}} - \frac{a_y H \delta^0_\rho (y-z)_\alpha}{2(y-z)^{2D-2}} + \frac{a_y a_z H^2 \delta^0_\rho \delta^0_\alpha}{4(y-z)^{2D-4}} \right\} \\ & = \frac{\Gamma\left(\frac{D}{2}-1\right)\mu^{D-4}}{32\pi^{\frac{D}{2}}(D-3)(D-4)} \left\{ \partial_\rho^y \partial_\alpha^z \left[\frac{i\delta^D(y-z)}{(a_y a_z)^{D-2}} \right] + \frac{[\partial_\rho^y \partial_\alpha^y - \eta_{\rho\alpha}\partial_y^2] i\delta^D(y-z)}{(D-1)(a_y a_z)^{D-2}} \right\} + (\text{Finite}). \end{aligned} \tag{A7}$$

We now extract derivatives from the last term in (A4),

$$-\frac{\Gamma(\frac{D}{2})\Gamma(\frac{D}{2}+1)H^2}{8\pi^D(a_y a_z)^{D-3}}\times\frac{(y-z)_\rho(y-z)_\alpha}{(y-z)^{2D-2}}$$
$$=-\frac{\Gamma(\frac{D}{2}-1)\Gamma(\frac{D}{2}+1)H^2}{32\pi^D(a_y a_z)^{D-3}}$$
$$\times\left[\frac{\partial_\rho^y\partial_\alpha^y}{2(D-3)}+\frac{\eta_{\rho\alpha}\partial_y^2}{2(D-3)(D-4)}\right]\frac{1}{(y-z)^{2D-6}}. \quad \text{(A8)}$$

Of the two terms inside the square brackets at the end of (A8), only the one proportional to $\eta_{\rho\alpha}\partial_y^2$ is divergent. Using the same reduction as (A6) we therefore reduce the last term of expression (A4) to

$$-\frac{\Gamma(\frac{D}{2})\Gamma(\frac{D}{2}+1)H^2}{8\pi^D(a_y a_z)^{D-3}}\times\frac{(y-z)_\rho(y-z)_\alpha}{(y-z)^{2D-2}}$$
$$=-\frac{\Gamma(\frac{D}{2}+1)}{16\pi^{\frac{D}{2}}}\frac{\mu^{D-4}\eta_{\rho\alpha}H^2 i\delta^D(y-z)}{(D-3)(D-4)(a_y a_z)^{D-3}}+(\text{Finite}). \quad \text{(A9)}$$

We are now ready to employ expressions (A7) and (A9) in (A1). Note that the transverse projection operator in the second term of (A7) vanishes upon canceling the scale factors and exploiting the $i\delta^D(y-z)$ to reflect derivatives where necessary,

$$\frac{\lambda^3}{4}\partial_y^\rho\partial_z^\alpha\left\{(a_y a_z)^{D-2}\frac{\Gamma(\frac{D}{2}-1)\mu^{D-4}}{32\pi^{\frac{D}{2}}(D-3)(D-4)}\frac{[\partial_\rho^y\partial_\alpha^y-\eta_{\rho\alpha}\partial_y^2]i\delta^D(y-z)}{(D-1)(a_y a_z)^{D-2}}\left[\delta^D(x-y)+\delta^D(x-z)\right]\right\}$$
$$=\frac{\lambda^3\mu^{D-4}\Gamma(\frac{D}{2}-1)\partial_y^\rho\partial_z^\alpha}{128\pi^{\frac{D}{2}}(D-1)(D-3)(D-4)}\left\{\left[\partial_\rho^z\partial_\alpha^z-\eta_{\rho\alpha}\partial_z^2\right]i\delta^D(y-z)\times\delta^D(x-y)\right.$$
$$\left.+\left[\partial_\rho^y\partial_\alpha^y-\eta_{\rho\alpha}\partial_y^2\right]i\delta^D(y-z)\times\delta^D(x-z)\right\}=0. \quad \text{(A10)}$$

The divergent part of $I(x;y;z)$ comes from the first term of (A7) and from (A8). After some judicious partial integrations it can be written as

$$I_{\rm div}=\frac{i\lambda^3\mu^{D-4}\Gamma(\frac{D}{2}-1)}{128\pi^{\frac{D}{2}}(D-3)(D-4)}\left\{2\mathcal{D}_y\mathcal{D}_z\left[\frac{\delta^D(x-y)\delta^D(x-z)}{(a_y a_z)^{D-2}}\right]-\mathcal{D}_y\partial_z^\alpha\left[\frac{\delta^D(y-z)\partial_\alpha^z\delta^D(x-z)}{a_y^{D-2}}\right]\right.$$
$$\left.-\mathcal{D}_z\partial_y^\rho\left[\frac{\delta^D(y-z)\partial_\rho^y\delta^D(x-y)}{a_z^{D-2}}\right]\right\}-\frac{i\lambda^3H^2a_x^2\mu^{D-4}\Gamma(\frac{D}{2}+1)}{32\pi^{\frac{D}{2}}(D-3)(D-4)}\partial_x^\mu\delta^D(x-y)\partial_\mu^x\delta^D(x-z). \quad \text{(A11)}$$

APPENDIX B: PARAMETERS AND VARIABLES

The aim of this appendix is to list all the parameters and variables used in the paper.

In Sec. I, we introduce scale factor $a(t)$, Hubble parameter $H(t)$, and first slow-roll parameter $\epsilon(t)$ in (1). In the same section, variables t, r, and k are comoving time, comoving coordinate distance to a point source, and plane wave number, respectively, given in (2) and (3). Moreover, G denotes Newton's constant of gravitation. In Sec. II, we introduce our model. A and B denote two scalar fields, and the model is given in (8). λ denotes the dimensionful coupling constant of our model. In (10) and (11), the coefficients C_{1A^2}, C_{2A^2}, C_{1B^2}, C_{2A^2}, C_{1AB^2},C_{2AB^2}, C_{3AB^2}, and C_{4AB^2} are counterterms. Also, D denotes the spacetime dimension and μ is the scale of the dimensional regularization. In the same section, we define the kinetic operator $\mathcal{D}$ in (12), and provide the scalar propagator $i\Delta(x:x')$ for fields A and B in (13). It should be noted that k does not denote the wave number in the rest of the paper, but is defined as a function of the Hubble parameter in (13). The notation adopted in the paper is summarized in the last paragraph of this section. In Sec. II, the contribution of each diagram in Fig. 4 to the expectation value of A is labeled A_{2a} through A_{2h}, and the results are given in (24) and (25). Furthermore, we provide the explicit form of 3-point and 4-point contributions to 1PI 2-loop functions $-iM_A^2(x;x')$ and $-iM_B^2(x;x')$ in (27) through (33). In the same section, β denotes the beta function for the field A, and it is defined in (36). Last, in Sec. IV, $\mathcal{A}$ denotes the stochastic random field. In (66) and (67), we provide the expressions for field strength renormalizations and gamma functions. They are denoted by Z and γ, respectively. $G(x_1;x_2;\ldots;x_n;\lambda;\mu)$ denotes the n-point Green function, the first time appearing in (68).

[1] V. F. Mukhanov and G. V. Chibisov, JETP Lett. **33**, 532 (1981).
[2] A. A. Starobinsky, JETP Lett. **30**, 682 (1979).
[3] L. Tan, N. C. Tsamis, and R. P. Woodard, Phil. Trans. R. Soc. A **380**, 0187 (2021).
[4] L. Tan, N. C. Tsamis, and R. P. Woodard, Universe **8**, 376 (2022).
[5] S. P. Miao and R. P. Woodard, Phys. Rev. D **74**, 024021 (2006).
[6] D. Glavan, S. P. Miao, T. Prokopec, and R. P. Woodard, Classical Quantum Gravity **31**, 175002 (2014).
[7] C. L. Wang and R. P. Woodard, Phys. Rev. D **91**, 124054 (2015).
[8] D. Glavan, S. P. Miao, T. Prokopec, and R. P. Woodard, J. High Energy Phys. 03 (2022) 088.
[9] N. C. Tsamis and R. P. Woodard, Nucl. Phys. **B724**, 295 (2005).
[10] H. Kitamoto and Y. Kitazawa, Phys. Rev. D **83**, 104043 (2011).
[11] H. Kitamoto and Y. Kitazawa, Phys. Rev. D **85**, 044062 (2012).
[12] H. Kitamoto, Phys. Rev. D **100**, 025020 (2019).
[13] A. A. Starobinsky, Lect. Notes Phys. **246**, 107 (1986).
[14] A. A. Starobinsky and J. Yokoyama, Phys. Rev. D **50**, 6357 (1994).
[15] S. P. Miao, N. C. Tsamis, and R. P. Woodard, J. High Energy Phys. 03 (2022) 069.
[16] R. P. Woodard and B. Yesilyurt, J. High Energy Phys. 06 (2023) 206.
[17] E. Kasdagli, M. Ulloa, and R. P. Woodard, Phys. Rev. D **107**, 105023 (2023).
[18] R. P. Woodard and B. Yesilyurt, J. High Energy Phys. 08 (2023) 124.
[19] H. J. Borchers, Nuovo Cimento (1955–1965) **15**, 784 (1960).
[20] N. N. Bogoliubov and O. S. Parasiuk, Acta Math. **97**, 227 (1957).
[21] K. Hepp, Commun. Math. Phys. **2**, 301 (1966).
[22] W. Zimmermann, Commun. Math. Phys. **11**, 1 (1968).
[23] W. Zimmermann, Commun. Math. Phys. **15**, 208 (1969).
[24] V. K. Onemli and R. P. Woodard, Classical Quantum Gravity **19**, 4607 (2002).
[25] V. K. Onemli and R. P. Woodard, Phys. Rev. D **70**, 107301 (2004).
[26] N. C. Tsamis and R. P. Woodard, Phys. Rev. D **69**, 084005 (2004).
[27] D. J. Brooker, N. C. Tsamis, and R. P. Woodard, Phys. Rev. D **96**, 103531 (2017).
[28] B. Losic and W. G. Unruh, Phys. Rev. D **71**, 044011 (2005).
[29] B. Losic and W. G. Unruh, Phys. Rev. D **72**, 123510 (2005).
[30] B. Losic and W. G. Unruh, Phys. Rev. D **74**, 023511 (2006).
[31] W. G. Unruh and B. Losic, Classical Quantum Gravity **25**, 154012 (2008).
[32] B. Losic and W. G. Unruh, Phys. Rev. Lett. **101**, 111101 (2008).